Article

NASH limits anti-tumour surveillance in immunotherapy-treated HCC

https://doi.org/10.1038/s41586-021-03362-0

Received: 17 February 2020

Accepted: 16 February 2021

Published online: 24 March 2021

Open access

Check for updates

Hepatocellular carcinoma (HCC) can have viral or non-viral causes[1–5]. Non-alcoholic steatohepatitis (NASH) is an important driver of HCC. Immunotherapy has been approved for treating HCC, but biomarker-based stratification of patients for optimal response to therapy is an unmet need[6,7]. Here we report the progressive accumulation of exhausted, unconventionally activated $CD8^+PD1^+$ T cells in NASH-affected livers. In preclinical models of NASH-induced HCC, therapeutic immunotherapy targeted at programmed death-1 (PD1) expanded activated $CD8^+PD1^+$ T cells within tumours but did not lead to tumour regression, which indicates that tumour immune surveillance was impaired. When given prophylactically, anti-PD1 treatment led to an increase in the incidence of NASH–HCC and in the number and size of tumour nodules, which correlated with increased hepatic $CD8^+PD1^+CXCR6^+$, TOX^+, and TNF^+ T cells. The increase in HCC triggered by anti-PD1 treatment was prevented by depletion of $CD8^+$ T cells or TNF neutralization, suggesting that $CD8^+$ T cells help to induce NASH–HCC, rather than invigorating or executing immune surveillance. We found similar phenotypic and functional profiles in hepatic $CD8^+PD1^+$ T cells from humans with NAFLD or NASH. A meta-analysis of three randomized phase III clinical trials that tested inhibitors of PDL1 (programmed death-ligand 1) or PD1 in more than 1,600 patients with advanced HCC revealed that immune therapy did not improve survival in patients with non-viral HCC. In two additional cohorts, patients with NASH-driven HCC who received anti-PD1 or anti-PDL1 treatment showed reduced overall survival compared to patients with other aetiologies. Collectively, these data show that non-viral HCC, and particularly NASH–HCC, might be less responsive to immunotherapy, probably owing to NASH-related aberrant T cell activation causing tissue damage that leads to impaired immune surveillance. Our data provide a rationale for stratification of patients with HCC according to underlying aetiology in studies of immunotherapy as a primary or adjuvant treatment.

Potentially curative treatments for HCC, such as liver transplantation, tumour resection, or ablation, are limited to early-stage tumours[1,2]. Multikinase inhibitors and anti-VEGF-R2 antibodies have been approved for use in advanced HCC[1,2]. Immunotherapy, which is thought to activate T cells or reinvigorate immune surveillance against cancer, showed response rates of 15–30% in patients with HCC[5,8–11]. Nivolumab and pembrolizumab (PD1-directed antibodies) have been approved for treatment of HCC[3,4], although phase III trials failed to reach their primary endpoints to increase survival[1,10,11]. A combination of atezolizumab (anti-PDL1) and bevacizumab (anti-VEGF) demonstrated increased overall and progression-free survival in a phase III trial, making it a first-line treatment for advanced HCC[5]. The efficacy of immunotherapy might be affected by different underlying HCC aetiologies, with diverse hepatic environments distinctly regulating HCC induction and immune responses[6]. Hence, we lack biomarkers that correlate with treatment response to allow patient stratification[12,13]. Non-alcoholic fatty liver disease (NAFLD) is an HCC-causing condition that affects more than 200 million people worldwide[14]. Approximately 10–20% of individuals with NAFLD progress over time from steatosis to NASH[14]. Innate and adaptive immune-cell activation[15–17], in combination with increased metabolites and endoplasmic reticulum stress[16,18], are believed to lead to a cycle of hepatic necro-inflammation and regeneration that potentially leads to HCC[19–21]. NASH has become an emerging risk factor for HCC[1,14,19], which led us to investigate the effects of immunotherapy in NASH–HCC[22–24].

Hepatic $CD8^+PD1^+$ T cells increase in NASH

We fed mice with diets that cause progressive liver damage and NASH over 3–12 months (Extended Data Fig. 1a–c), accompanied by an increase in the frequency of activated $CD8^+$ T cells expressing CD69, CD44 and PD1 (Extended Data Fig. 1d–g). Single-cell mapping of leukocytes showed altered immune-cell compositions in mice with NASH (Extended Data Fig. 1h, i) with strongly increased numbers of $CD8^+PD1^+$ cells (Fig. 1a, b, Extended Data Fig. 1j–m, o). Similarly, elevated $CD8^+$ and $PD1^+$ cells were found in a genetic mouse model of NASH[17] (Extended Data Fig. 1n). Messenger RNA in situ hybridization and immunohistochemistry showed that increasing PDL1 expression in hepatocytes and

A list of authors and their affiliations appears online. ✉e-mail: m.heikenwaelder@dkfz-heidelberg.de

non-parenchymal cells correlated with the severity of NASH (Extended Data Fig. 1p). Mass spectrometric characterization of $CD8^+PD1^+$ T cells from NASH-affected livers indicated enrichment in pathways involved in ongoing T cell activation and differentiation, TNF signalling, and natural killer (NK) cell-like cytotoxicity (Fig. 1c). Single-cell RNA sequencing (scRNA-seq) of cells expressing T cell receptor β-chains (TCRβ) from the livers of mice with NASH showed that $CD8^+$ T cells had gene expression profiles related to cytotoxicity and effector-function (for example, *Gzmk* and *Gzmm)* and inflammation markers (for example, *Ccl3*) with elevated exhaustion traits (for example, *Pdcd1* and *Tox*) (Fig. 1d, e). RNA-velocity analyses demonstrated enhanced transcriptional activity and differentiation from *Sell*-expressing $CD8^+$ to $CD8^+PD1^+$ T cells (Extended Data Fig. 1q), indicating local differentiation. Thus, mice with NASH have increased hepatic abundance of $CD8^+PD1^+$ T cells with features of exhaustion and effector functions.

The high numbers of T cells in NASH suggest that anti-PD1-targeted immunotherapy may serve as an efficient therapy for NASH–HCC. Thirty per cent of C57BL/6 mice fed a choline-deficient high-fat diet (CD-HFD) for 13 months developed liver tumours with a similar load of genetic alterations to human NAFLD–HCC or NASH–HCC (Extended Data Fig. 2a, b). NASH mice bearing HCC (identified using MRI) were allocated to anti-PD1 immunotherapy or control arms (Fig. 1f). None of the pre-existing liver tumours regressed in response to anti-PD1 therapy (Fig. 1g, h, Extended Data Fig. 2c). Rather, we observed increased fibrosis, unchanged liver damage, slightly increased incidence of liver cancer and unaltered tumour loads and sizes after anti-PD1 treatment (Extended Data Fig. 2 d–h). In anti-PD1-treated mice, liver tumour tissue contained increased numbers of $CD8^+/PD1^+$ T cells and high levels of cells expressing *Cxcr6* or *Tnf* mRNA (Extended Data Fig. 2i–n). We found no regression of NASH-induced liver tumours upon anti-PDL1 immunotherapy (Extended Data Fig. 3a–f). By contrast, other (non-NASH) mouse models of liver cancer (with or without concomitant damage) reacted to PD1 immunotherapy with tumour regression[25], suggesting that lack of response to immunotherapy was associated specifically with NASH–HCC (Extended Data Fig. 3g–i). Thus, NASH precluded efficient anti-tumour surveillance in the context of HCC immunotherapy. Similarly, impaired immunotherapy has been described in mouse models with NASH and secondary liver cancer[25,26].

$CD8^+$ T cells promote HCC in NASH

As $CD8^+PD1^+$ T cells failed to execute effective immune surveillance, but rather showed tissue-damaging potential, we reasoned that $CD8^+$ T cells might be involved in promoting NASH–HCC. We depleted $CD8^+$ T cells in a preventive setting in mice with NASH but without liver cancer (CD-HFD fed for 10 months). $CD8^+$ T cell depletion significantly decreased liver damage and the incidence of HCC in these mice (Fig. 2i, Extended Data Fig. 4a–j, n). Similar results were obtained after co-depletion of $CD8^+$ and $NK1.1^+$ cells (Fig. 2i, Extended Data Fig. 4a–f, n). This suggests that as well as lacking immune surveillance functions, liver $CD8^+$ T cells also promote HCC in mice with NASH. Next, we investigated the effect of anti-PD1 therapy on HCC development in mice with NASH. Anti-PD1 immunotherapy aggravated liver damage (Fig. 2g, Extended Data Fig. 7c) and increased hepatic $CD8^+PD1^+$ T cells, with only minor changes in liver $CD4^+PD1^+$ T cells or other immune-cell populations (Extended Data Fig. 4a–o). Anti-PD1 immunotherapy also caused a marked increase in liver-cancer incidence, independent of changes in liver fibrosis (Fig. 2i). Mice lacking PD1 ($Pdcd1^{-/-}$) showed an increase in incidence of, and earlier onset of, liver cancer, along with increased liver damage and elevated numbers of activated hepatic $CD8^+$ T cells with increased cytokine expression (IFNγ, TNF) (Extended Data Fig. 5a–g). In summary, $CD8^+PD1^+$ T cells triggered the transition to HCC in mice with NASH, probably owing to impaired tumour surveillance and enhanced T cell-mediated tissue damage[27]. Despite a strong increase in $CD8^+PD1^+$ T cells within tumours, therapeutic PD1- or PDL1-related immunotherapy failed to cause tumour regression in NASH–HCC.

We used an immune-mediated cancer field (ICF) gene-expression signature associated with the development of human HCC[28] to understand the tumour-driving mechanisms of anti-PD1 immunotherapy. Preventive anti-PD1 treatment was strongly associated with the pro-tumorigenic immunosuppressive ICF signature (for example, *Ifng*, *Tnf*, *Stat3*, *Tgfb1*), capturing the traits of T cell exhaustion, pro-carcinogenic signalling, and mediators of immune tolerance and inhibition. Depletion of $CD8^+$ T cells led to significant downregulation of the high-infiltrate ICF signature and diminished TNF in non-parenchymal cells (Extended Data Fig. 5h, i). Gene set enrichment analysis (GSEA), mRNA in situ hybridization, and histology of tumours developed in NASH mice that were treated prophylactically with anti-PD1 corroborated these data, showing increased $CD8^+$ T cell abundance and enrichment for genes involved in inflammation-related signalling, apoptosis, and TGFβ signalling (Extended Data Fig. 5j–l). Anti-PD1 treatment triggered the expression of p62 (Extended Data Fig. 5m), which has been shown to drive hepatocarcinogenesis[29]. Array comparative genomic hybridization identified no significant differences in chromosomal deletions or amplifications between tumours from anti-PD1-treated mice or control mice (Extended Data Fig. 5n). In summary, hepatic $CD8^+PD1^+$ T cells did not cause tumour regression during NASH, but rather were linked to HCC development, which was enhanced by anti-PD1 immunotherapy.

We next analysed the hepatic T cell compartment for correlations with inflammation and hepatocarcinogenesis. Comparison of $CD8^+PD1^+$ T cells with $CD8^+$ T cells by scRNA-seq showed that the former showed higher expression of genes associated with effector function (for example, increased *Gzma*, *Gzmb*, *Gzmk*, *Prf1*; reduced *Sell*, *Klf2*), exhaustion (for example, increased *Pdcd1*, *Tox*; reduced *Il7r*, *Tcf7*) and tissue residency (for example, increased *Cxcr6*, low levels of Ki-67) (Extended Data Fig. 6a–c). Notably, there was no difference in the transcriptome profiles of $CD8^+PD1^+$ T cells in NASH mice after anti-PD1 immunotherapy (Extended Data Fig. 6c), indicating that the number of T cells rather than their functional properties were changed. RNA-velocity blot analyses corroborated these data (Fig. 2a, Extended Data Fig. 6d–f). Similar patterns of markers (for example, *IL7r*, *Sell*, *Tcf7*, *Ccl5*, *Pdcd1*, *Cxcr6*, and *Rgs1*) correlated with latent time and overall transcriptional activity in NASH mice that received either treatment (Fig. 2a, b, Extended Data Fig. 6e, f). Mass spectrometry-based analyses of $CD8^+$ or $CD8^+PD1^+$ T cells isolated from NASH mouse livers confirmed these findings (Fig. 2c, Extended Data Fig. 6g).

We characterized the transcriptome profiles of $PD1^+CD8^+$ T cells by uniform manifold approximation and projection (UMAP) analysis of high-parametric flow-cytometry data, dissecting the $CD8^+PD1^+$ and $CD8^+PD1^-$ subsets (Fig. 2d). This revealed that $CD8^+PD1^+$ cells expressed high levels of effector (for example, *Gzmb*, *Ifng*, *Tnf*) and exhaustion markers (for example, *Eomes*, *Pdcd1*, Ki-67^{low}). In particular, $CD8^+PD1^+TNF^+$ cells were more abundant upon anti-PD1 treatment (Fig. 2e). Convolutional neural network analysis and manual gating validated this result (Fig. 2f, Extended Data Fig. 6j, k). $CD8^+PD1^+$ T cells were non-proliferative in anti-PD1-treated NASH mice; this result was supported by in vitro experiments, in which anti-PD1 treatment led to increased T cell numbers in the absence of proliferation (Extended Data Fig. 6l, m). Notably, $CD8^+PD1^+$ T cells from NASH mice showed reduced levels of FOXO1, which indicates an enhanced tissue-residency phenotype[30], potentially combined with boosted effector function, as indicated by higher calcium levels in $CD8^+PD1^+$ T cells (Extended Data Fig. 6n, o). Single-cell RNA-seq analysis also showed that $CD8^+PD1^+$ T cells from NASH mice had a tissue residency signature (Extended Data Fig. 6b). Thus, upon anti-PD1 immunotherapy in NASH mice, $CD8^+PD1^+$ T cells accumulated to high numbers in the liver, revealing a resident-like T cell character with increased expression of CD44, CXCR6, EOMES and TOX and low levels of CD244

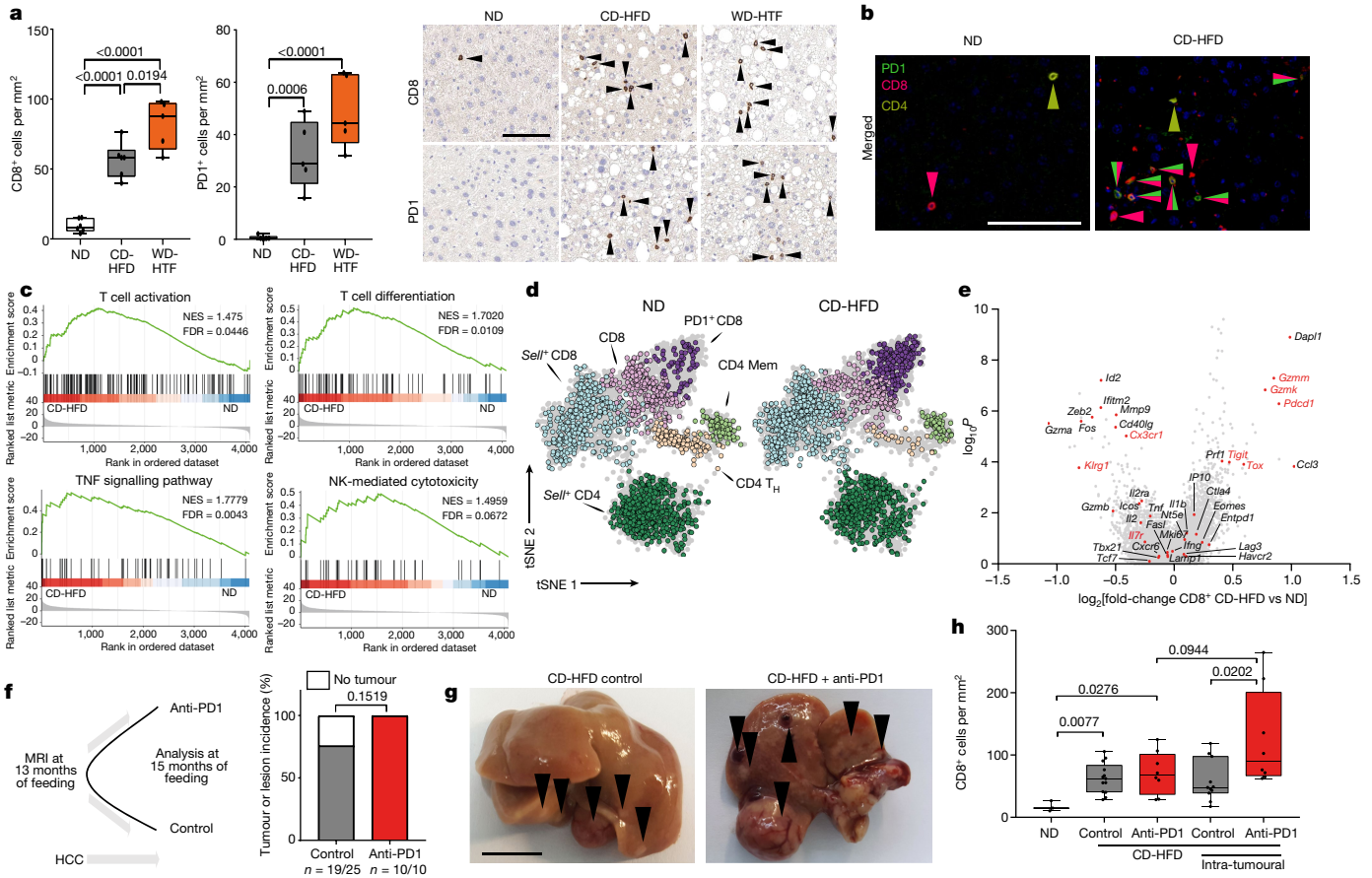

Fig. 1 | NASH progression is associated with increased, activated CD8$^+$PD1$^+$ T cells. a, CD8 and PD1 staining (right) and quantification (left) of T cells from mice fed normal diet (ND), CD-HFD or western-style diet with trans fat (WD-HTF) by immunohistochemistry. **b**, Immunofluorescence-based detection of PD1 (green), CD8 (red) and CD4 (yellow) cells. Scale bar, 100 µm. **c**, GSEA of hepatic CD8$^+$PD1$^+$ T cells sorted from TCRβ$^+$ cells by mass spectrometry. FDR, false discovery rate; NES, normalized enrichment score. **d**–**f**, *t*-distributed stochastic neighbour embedding (tSNE) of TCRβ$^+$ cells (**d**), differential gene expression by scRNA-seq (**e**) and scheme for experiment (**f**): mice were fed CD-HFD for 13 months and then treated with anti-PD1 for 8 weeks before measurement of tumour incidence. Mem, memory CD4 T cells. **g**, Livers from treated and untreated mice after CD-HFD. Arrowheads, tumours or lesions. Scale bar, 10 mm. **h**, Quantification of CD8$^+$ cell in liver by immunohistochemistry. Details of sample sizes, biological replicates and statistical tests are given in Methods and Source Data. **a**, **h**, *P* values shown above brackets.

expression, but lacking expression of TCF1/TCF7, CD62L, TBET, and CD127 (Extended Data Fig. 6p–u). In summary, anti-PD1 immunotherapy increased the abundance of CD8$^+$PD1$^+$ T cells with a residency signature in the liver.

To investigate the mechanisms that drive the increased NASH–HCC transition in the preventive anti-PD1 treatment-setting, we treated NASH-affected mice with combinations of treatments. Both anti-CD8–anti-PD1 and anti-TNF–anti-PD1 antibody treatments ameliorated liver damage, liver pathology and liver inflammation (Fig. 2g, Extended Data Fig. 7), and decreased the incidence of liver cancer compared to anti-PD1 treatment alone (Fig. 2i). By contrast, anti-CD4–anti-PD1 treatment did not reduce the incidence of liver cancer, the NAFLD activity score (NAS), or the number of TNF-expressing hepatic CD8$^+$ or CD8$^+$PD1$^+$CXCR6$^+$ T cells (Fig. 2g–i, Extended Data Fig. 7). However, both the number of tumours per liver and tumour size were reduced, suggesting that depletion of CD4$^+$ T cells or regulatory T cells might contribute to tumour control (Extended Data Fig. 8a, b). The incidence of tumours was directly correlated with anti-PD1 treatment, alanine aminotransferase (ALT), NAS, number of hepatic CD8$^+$PD1$^+$ T cells, and TNF expression (Extended Data Fig. 8c–e). These data suggested that CD8$^+$PD1$^+$ T cells lacked immune-surveillance and had tissue-damaging functions[27], which were increased by anti-PD1 treatment, possibly contributing to the unfavourable effects of anti-PD1 treatment on HCC development in NASH.

Augmented CD8$^+$PD1$^+$ T cells in human-NASH

We next investigated CD8$^+$ T cells from healthy or NAFLD/NASH-affected livers. In two independent cohorts of patients with NASH, we found enrichment of hepatic CD8$^+$PD1$^+$ T cells with a residency phenotype (by flow cytometry and mass cytometry) (Fig. 3a, b, Extended Data Fig. 9a–j, Supplementary Tables 1,2). The number of hepatic CD8$^+$PD1$^+$ T cells directly correlated with body-mass index and liver damage (Extended Data Fig. 9b). To investigate similarities between mouse and human T cells from livers with NASH, we analysed liver CD8$^+$PD1$^+$ T cells from patients with NAFLD or NASH by scRNA-seq. This identified a gene expression signature that was also found in liver T cells from NASH mice (for example, *PDCD1*, *GZMB*, *TOX*, *CXCR6*, *RGS1*, *SELL*) (Fig. 3c, d, Extended Data Fig. 9k, l). Differentially expressed genes were directly correlated between patient- and mouse-derived hepatic CD8$^+$PD1$^+$ T cells (Fig. 3d). Velocity-blot analyses identified CD8$^+$ T cells expressing *TCF7*, *SELL* and *IL7R* as root cells, and CD8$^+$PD1$^+$ T cells as their endpoints (Fig. 3e, f), indicating a local developmental trajectory of CD8$^+$ T cells into CD8$^+$PD1$^+$ T cells. The amount of gene expression and velocity magnitude, which indicate transcriptional activity, were increased in CD8$^+$PD1$^+$ T cells from mice and humans with NASH (Fig. 3e). The expression of specific marker genes (for example, *IL7R*, *SELL*, *TCF7*, *CCL5*, *CCL3*, *PDCD1*, *CXCR6*, *RGS1* and *KLF2*) along the latent time in patients with NAFLD or NASH differed from that seen in control participants

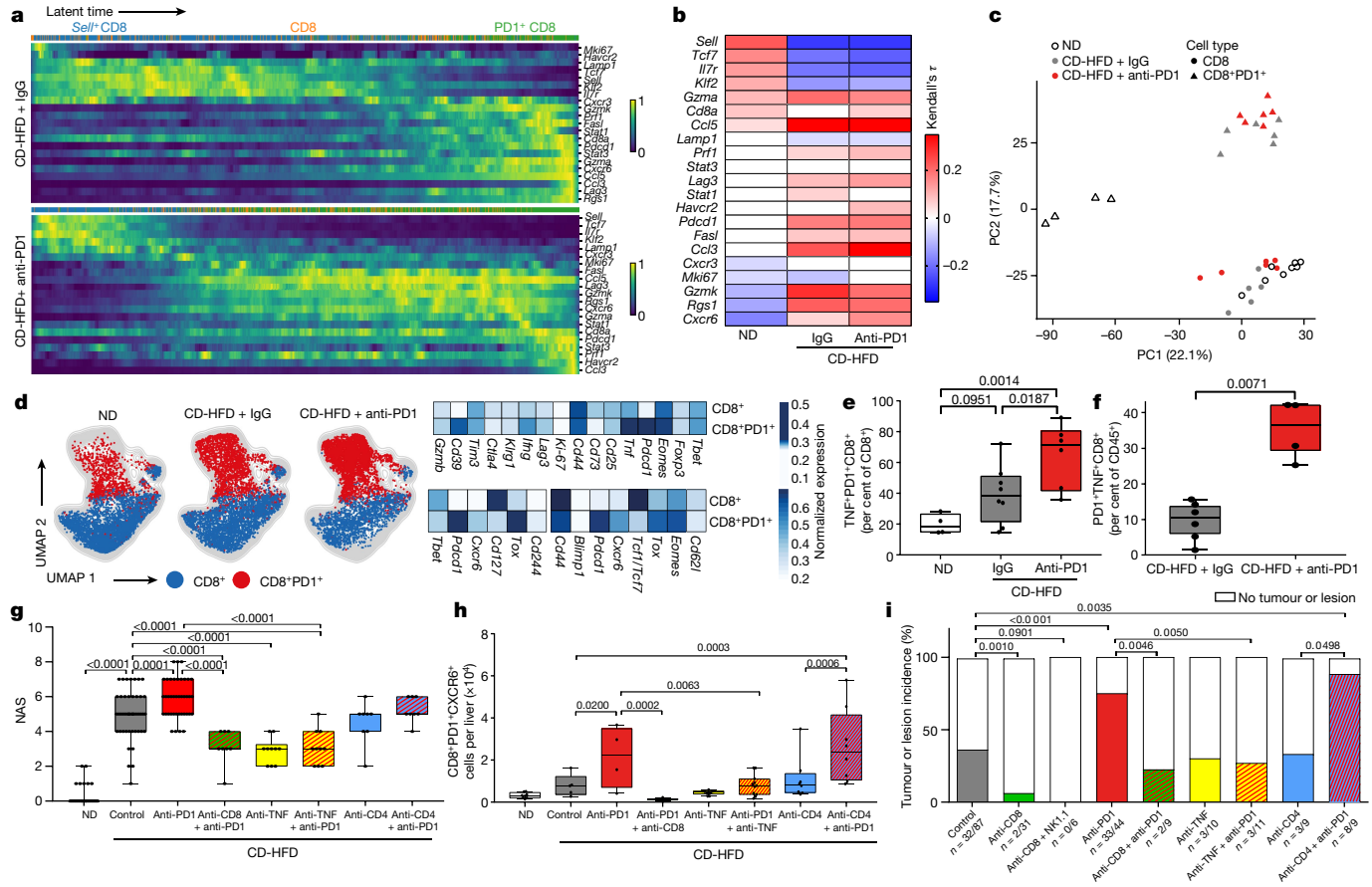

Fig. 2 | Resident-like CD8⁺PD1⁺ T cells drive hepatocarcinogenesis in a TNF-dependent manner upon anti-PD1 treatment in NASH. **a**, **b**, RNA-velocity analyses of scRNA-seq data showing expression (**a**) and correlation of expression (**b**) along the latent time of selected genes in CD8⁺ T cells from mice with NASH. Latent time (pseudo-time by RNA velocity): dark colour, start of RNA velocity; yellow, end point of latent time. Kendall's τ, gene expression along latent time. **c**, Principal component analysis (PCA) plot of hepatic CD8⁺ and CD8⁺PD1⁺ T cells sorted by mass spectrometry from TCRβ⁺ cells from mice fed for 12 months with ND, CD-HFD or CD-HFD and treated for 8 weeks with anti-PD1 antibodies. **d**, **e**, UMAP representations showing FlowSOM-guided clustering (**d**, left), heat map showing median marker expression (**d**, right), and quantification of hepatic CD8⁺ T cells (**e**) from mice fed for 12 months with ND or CD-HFD and treated for 8 weeks with IgG or anti-PD1 antibodies. **f**, Quantification of CellCNN-analysed flow cytometry data for hepatic CD8⁺ T cells from mice fed for 12 months with CD-HFD and treated for 8 weeks with IgG or anti-PD1 antibodies. **g**, **h**, NAS evaluation (**g**) and quantification of hepatic CD8⁺PD1⁺CXCR6⁺ T cells (**h**) from mice fed with ND for 12 months or fed with CD-HFD for 12 months and treated for 8 weeks with anti-PD1, anti-PD1 + anti-CD8, anti-TNF, anti-PD1 + anti-TNF, anti-CD4, or anti-PD1 + anti-CD4 antibodies. Kendall's τ, gene expression along latent time. **i**, Quantification of tumour incidence in mice as in **g**, **h**. Details of sample sizes, biological replicates and statistical tests are given in Methods and Source Data. **e**–**i**, *P* values shown above brackets.

(Fig. 3g), and correlated with the expression patterns seen in CD8⁺ T cells from NASH mice (Fig. 3h). Thus, scRNA-seq analysis demonstrated a resident-like liver CD8⁺PD1⁺ T cell population in patients with NAFLD or NASH that shared gene expression patterns with hepatic CD8⁺PD1⁺ T cells from NASH mice.

Different stages of NASH severity are considered to herald the development of liver cancer[31]. Indeed, different fibrosis stages (F0–F4) in patients with NASH correlated directly with the expression of *PDCD1*, *CCL2*, *IP10* and *TNF*, and the degree of fibrosis correlated with the numbers of CD4⁺, PD1⁺, and CD8⁺ T cells (Extended Data Fig. 10a–d, Supplementary Table 3). Moreover, PD1⁺ cells were absent from healthy livers but present in the livers of patients with NASH or NASH–HCC, but the number of these cells did not differ with the underlying fibrosis level (Extended Data Fig. 10e, Supplementary Tables 4–6). Species-specific effects, such as the absence in mice of cirrhosis or burnt-out NASH (a condition found in some patients with NASH–HCC[32]), and their possible influence on immunotherapy may make it difficult to translate findings from preclinical models of NASH to human NASH. However, in tumour tissue from patients with NASH-induced HCC—treated with anti-PD1 therapy—we found increased numbers of intra-tumoral PD1⁺ cells compared to patients with HCC and viral hepatitis (Extended Data Fig. 10f). Thus, we found a shared gene-expression profile and increased abundance of unconventionally activated hepatic CD8⁺PD1⁺ T cells in human NASH tissue.

Lack of immunotherapy response in human NASH–HCC

To explore the concept of disrupted immune surveillance in NASH after anti-PD1 or anti-PDL1 treatment, we conducted a meta-analysis of three large randomized controlled phase III trials of immunotherapies in patients with advanced HCC (CheckMate-459[11], IMbrave150[5] and KEYNOTE-240[10]). Although immunotherapy improved survival in the overall population (hazard ratio (HR) 0.77; 95% confidence interval (CI) 0.63–0.94), survival was superior to the control arm in patients with HBV-related HCC ($n = 574$; $P = 0.0008$) and HCV-related HCC ($n = 345$; $P = 0.04$), but not in patients with non-viral HCC ($n = 737$; $P = 0.39$) (Fig. 4a, Extended Data Fig. 10g, Supplementary Table 7). Patients with viral aetiology (HBV or HCV infection) of liver damage and HCC showed a benefit from checkpoint inhibition (HR 0.64; 95% CI 0.48–0.94), whereas patients with HCC of a non-viral aetiology

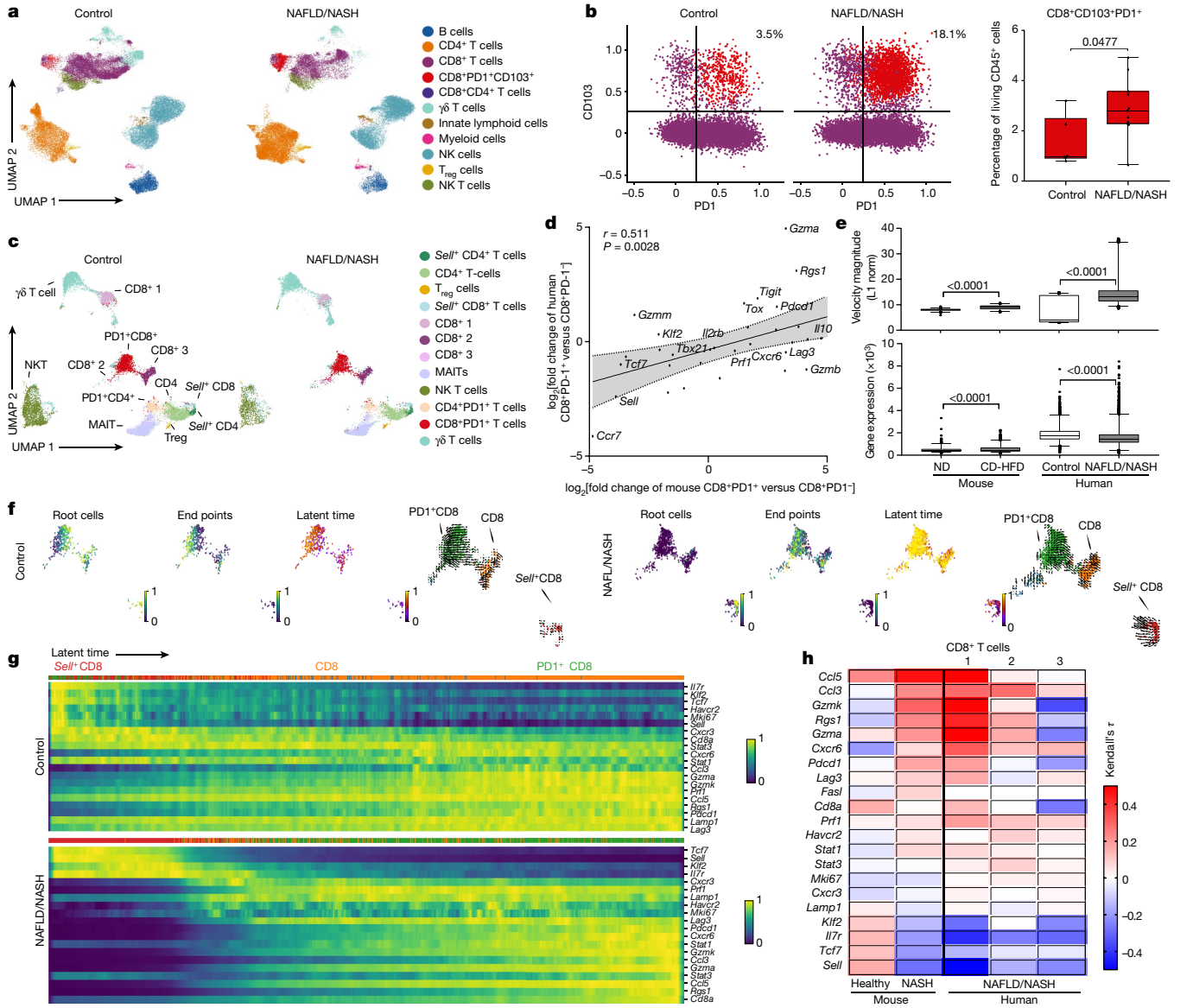

Fig. 3 | Hepatic resident-like CD8$^+$PD1$^+$ T cells are increased in livers of patients with NAFLD patients. a, **b**, UMAP representation showing the FlowSOM-guided clustering of CD45$^+$ cells (**a**) and flow cytometry plots (**b**, left) and quantification (**b**, right) of CD8$^+$PD1$^+$CD103$^+$ cells derived from hepatic biopsies of healthy individuals or patients with NAFLD or NASH (Supplementary Table 2). Populations in **b**: violet, CD8$^+$; red, CD8$^+$PD1$^+$CD103$^+$. T_{reg} cells, regulatory T cells. **c**, UMAP representations and analyses of differential gene expression by scRNA-seq of CD3$^+$ cells from control individuals or patients with NAFLD or NASH. MAITs, mucosal-associated invariant T cells. **d**, Correlation of significant differentially expressed genes in liver-derived CD8$^+$PD1$^+$ T cells compared to CD8$^+$PD1$^-$ T cells from mice fed with CD-HFD for 12 months and patients with NAFLD/NASH. Shading shows 95% CI. **e**–**h**, Expression (**e**) and transcriptional activity (**f**) of velocity analyses of scRNA-seq data, and gene expression (**g**) and correlation (**h**) of expression along the latent-time of selected genes along the latent-time of liver-derived CD8$^+$ T cells from patients with NAFLD or NASH in comparison to control or NASH mouse liver-derived CD8$^+$ T cells. Root cells: yellow, root cells; blue, cells furthest from the root by RNA velocity. End points: yellow, end-point cells; blue, cells furthest from defined end-point cells by RNA velocity. Latent time (pseudo-time by RNA velocity): dark colour, start of RNA velocity; yellow, end point of latent time. RNA velocity flow (top): blue cluster, start point; orange cluster, intermediate; green cluster, end point. Arrow indicates cell trajectory. Details of sample sizes, biological replicates and statistical tests are given in Methods and Source Data. **b**, **e**, *P* values shown above brackets.

did not (HR 0.92; 95% CI 0.77–1.11; *P* of interaction = 0.03 (Fig. 4a)). Subgroup analysis of first-line treatment compared to a control arm treated with sorafenib (n = 1,243) confirmed that immunotherapy was superior in patients with HBV-related (n = 473; P = 0.03) or HCV-related HCC (n = 281; P = 0.03), but not in patients with non-viral HCC (n = 489; P = 0.62; Extended Data Fig. 10h–j). We acknowledge that these results were derived from a meta-analysis of trials that included different lines of treatment and patients with heterogeneous liver damage, and did not differentiate between alcoholic liver disease and NAFLD or NASH. Nevertheless, the results of this meta-analysis supported the notion that stratification of patients according to the aetiology of their liver damage and ensuing HCC identified patients who responded well to therapy.

To specifically characterize the effect of anti-PD(L)1 immunotherapy with respect to underlying liver disease, we investigated a cohort of 130 patients with HCC (patients with NAFLD n = 13; patients with other aetiologies n = 117) (Supplementary Table 8). NAFLD was associated with shortened median overall survival after immunotherapy (5.4 months (95% CI 1.8–9.0 months) versus 11.0 months (95% CI 7.5–14.5 months); P = 0.023), even though patients with NAFLD had less frequent macrovascular tumour invasion (23% versus 49%), and immunotherapy was more often used as a first-line therapy in these patients (46% versus 23%;

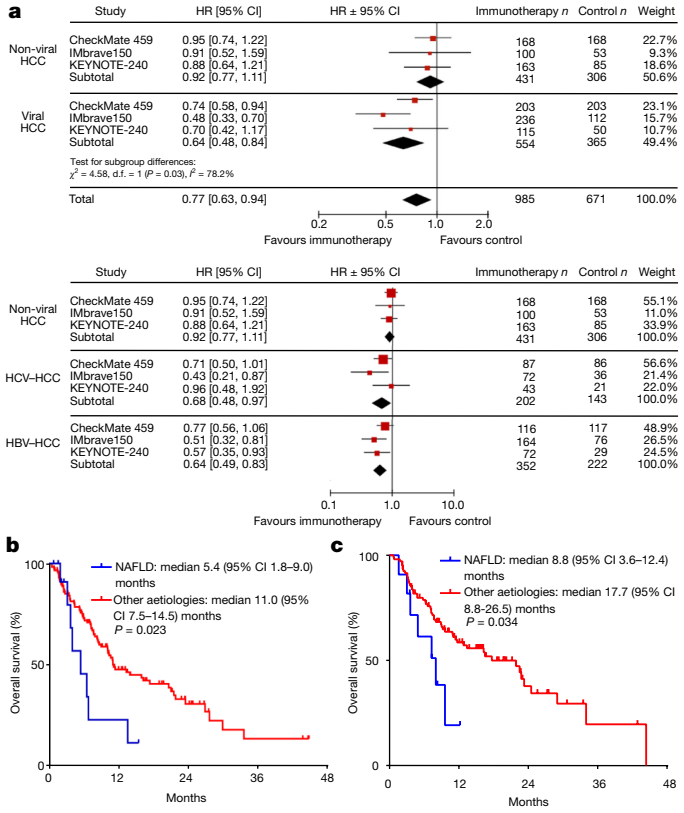

Fig. 4 | PD1 and PDL1 targeted immunotherapy in advanced HCC has a distinct effect depending on disease aetiology. a, Meta-analysis of 1,656 patients (Supplementary Table 7). Immunotherapy was initially assessed and then analysed according to disease aetiology: non-viral (NASH and alcohol intake) vs viral (HBV and HCV) (top). Heterogeneity: $\tau^2 = 0.00$; $\chi^2 = 0.14$, degrees of freedom (d.f.) = 2 ($P = 0.93$); $I^2 = 0\%$. Test for overall effect: $Z = 0.87$ ($P = 0.39$). Separate meta-analyses were subsequently performed for each of the three aetiologies: non-viral (NASH and alcohol intake), HCV and HBV (bottom). Heterogeneity: $\tau^2 = 0.03$; $\chi^2 = 3.67$, d.f. = 2 ($P = 0.16$); $I^2 = 46\%$. Test for overall effect: $Z = 3.13$ ($P = 0.002$). Diamonds represent estimated overall effect based on the meta-analysis random effect of all trials. Inverse variance and random effects methods were used to calculate HRs, 95% CIs, *P* values, and the test for overall effect; calculations were two-sided. **b**, NAFLD is associated with a worse outcome in patients with HCC treated with PD(L)1-targeted immunotherapy. A total of 130 patients with advanced HCC received PD(L)1-targeted immunotherapy (Supplementary Table 8). **c**, Validation cohort of patients with HCC treated with PD(L)1-targeted immunotherapy. A total of 118 patients with advanced HCC received PD(L)1-targeted immunotherapy (Supplementary Table 10). **b**, **c**, Log-rank test. Details of sample sizes, biological replicates and statistical tests are given in Methods and Source Data.

Fig. 4b). After correction for potentially confounding factors that are relevant for prognosis, including severity of liver damage, macrovascular tumour invasion, extrahepatic metastases, performance status, and alpha-fetoprotein (AFP), NAFLD remained independently associated with shortened survival of patients with HCC after anti-PD1-treatment (HR 2.6; 95% CI 1.2–5.6; $P = 0.017$, Supplementary Table 9). This finding was validated in a further cohort of 118 patients with HCC who were treated with PD(L)1-targeted immunotherapy (patients with NAFLD $n = 11$; patients with other aetiologies $n = 107$) (Supplementary Table 10). NAFLD was again associated with reduced survival of patients with HCC (median overall survival 8.8 months, 95% CI 3.6–12.4 months) compared to other aetiologies of liver damage (median overall survival 17.7 months, 95% CI 8.8–26.5 months; $P = 0.034$) (Fig. 4c). Given the relatively small number of patients with NAFLD in both cohorts, these data need prospective validation. However, collectively these results indicate that patients with underlying NASH did not benefit from checkpoint-inhibition therapy.

Liver cancer develops primarily on the basis of chronic inflammation. The latter can be activated by immunotherapy to induce tumour regression in a subset of patients with liver cancer. However, the identification of patients who will respond to immunotherapy for HCC remains difficult. Our data identify a non-viral aetiology of liver damage and cancer (that is, NASH) as a predictor of unfavourable outcome in patients treated with immune-checkpoint inhibitors. The better response to immunotherapy in patients with virus-induced HCC than in patients with non-viral HCC might be due to the amount or quality of viral antigens or to a different liver micro-environment, possibly one that does not impair immune surveillance. These results might also have implications for patients with obesity and NALFD or NASH who have cancer at other organ sites (for example, melanoma, colon carcinoma, or breast cancer) and are at risk for liver damage and the development of liver cancer in response to systemically applied immunotherapy. Overall, our results provide comprehensive mechanistic insight and a rational basis for the stratification of patients with HCC according to their aetiology of liver damage and cancer for the design of future trials of personalized cancer therapy.

Online content

Any methods, additional references, Nature Research reporting summaries, source data, Extended Data Fig., supplementary information, acknowledgements, peer review information; details of author contributions and competing interests; and statements of data and code availability are available at https://doi.org/10.1038/s41586-021-03362-0.

1. Llovet, J. M. et al. Hepatocellular carcinoma. *Nat. Rev. Dis. Primers* **7**, 6 (2021).
2. European Association for the Study of the Liver EASL Clinical Practice Guidelines: management of hepatocellular carcinoma. *J. Hepatol.* **69**, 182–236 (2018).
3. Zhu, A. X. et al. Pembrolizumab in patients with advanced hepatocellular carcinoma previously treated with sorafenib (KEYNOTE-224): a non-randomised, open-label phase 2 trial. *Lancet Oncol.* **19**, 940–952 (2018).
4. El-Khoueiry, A. B. et al. Nivolumab in patients with advanced hepatocellular carcinoma (CheckMate 040): an open-label, non-comparative, phase 1/2 dose escalation and expansion trial. *Lancet* **389**, 2492–2502 (2017).
5. Finn, R. S. et al. Atezolizumab plus bevacizumab in unresectable hepatocellular carcinoma. *N. Engl. J. Med.* **382**, 1894–1905 (2020).
6. Roderburg, C., Wree, A., Demir, M., Schmelzle, M. & Tacke, F. The role of the innate immune system in the development and treatment of hepatocellular carcinoma. *Hepatic Oncol.* **7**, HEP17 (2020).
7. Pinter, M., Scheiner, B. & Peck-Radosavljevic, M. Immunotherapy for advanced hepatocellular carcinoma: a focus on special subgroups. *Gut* **70**, 204–214 (2021).
8. Duffy, A. G. et al. Tremelimumab in combination with ablation in patients with advanced hepatocellular carcinoma. *J. Hepatol.* **66**, 545–551 (2017).
9. Sangro, B. et al. A clinical trial of CTLA-4 blockade with tremelimumab in patients with hepatocellular carcinoma and chronic hepatitis C. *J. Hepatol.* **59**, 81–88 (2013).
10. Finn, R. S. et al. Pembrolizumab as second-line therapy in patients with advanced hepatocellular carcinoma in KEYNOTE-240: a randomized, double-blind, phase III trial. *J. Clin. Oncol.* **38**, 193–202 (2020).
11. Yau, T. et al. CheckMate 459: A randomized, multi-center phase III study of nivolumab (NIVO) vs sorafenib (SOR) as first-line (1L) treatment in patients (pts) with advanced hepatocellular carcinoma (aHCC). *Ann. Oncol.* **30**, v874–v875 (2019).
12. van der Leun, A. M., Thommen, D. S. & Schumacher, T. N. $CD8^+$ T cell states in human cancer: insights from single-cell analysis. *Nat. Rev. Cancer* **20**, 218–232 (2020).
13. Sangro, B. et al. Association of inflammatory biomarkers with clinical outcomes in nivolumab-treated patients with advanced hepatocellular carcinoma. *J. Hepatol.* **73**, 1460–1469 (2020).
14. Anstee, Q. M., Reeves, H. L., Kotsiliti, E., Govaere, O. & Heikenwalder, M. From NASH to HCC: current concepts and future challenges. *Nat. Rev. Gastroenterol. Hepatol.* **16**, 411–428 (2019).
15. Wolf, M. J. et al. Metabolic activation of intrahepatic $CD8^+$ T cells and NKT cells causes nonalcoholic steatohepatitis and liver cancer via cross-talk with hepatocytes. *Cancer Cell* **26**, 549–564 (2014).
16. Ma, C. et al. NAFLD causes selective $CD4^+$ T lymphocyte loss and promotes hepatocarcinogenesis. *Nature* **531**, 253–257 (2016).
17. Malehmir, M. et al. Platelet GPIbα is a mediator and potential interventional target for NASH and subsequent liver cancer. *Nat. Med.* **25**, 641–655 (2019).
18. Nakagawa, H. et al. ER stress cooperates with hypernutrition to trigger TNF-dependent spontaneous HCC development. *Cancer Cell* **26**, 331–343 (2014).

19. Ringelhan, M., Pfister, D., O'Connor, T., Pikarsky, E. & Heikenwalder, M. The immunology of hepatocellular carcinoma. *Nat. Immunol.* **19**, 222–232 (2018).
20. Michelotti, G. A., Machado, M. V. & Diehl, A. M. NAFLD, NASH and liver cancer. *Nat. Rev. Gastroenterol. Hepatol.* **10**, 656–665 (2013).
21. Friedman, S. L., Neuschwander-Tetri, B. A., Rinella, M. & Sanyal, A. J. Mechanisms of NAFLD development and therapeutic strategies. *Nat. Med.* **24**, 908–922 (2018).
22. Wang, Z. et al. Paradoxical effects of obesity on T cell function during tumor progression and PD-1 checkpoint blockade. *Nat. Med.* **25**, 141–151 (2019).
23. Shalapour, S. et al. Inflammation-induced IgA^+ cells dismantle anti-liver cancer immunity. *Nature* **551**, 340–345 (2017).
24. Kim, C. G. et al. Hyperprogressive disease during PD-1 blockade in patients with advanced hepatocellular carcinoma. *J. Hepatol.* **74**, 350–359 (2021).
25. Chung, A. S. et al. Immune checkpoint inhibition is safe and effective for liver cancer prevention in a mouse model of hepatocellular carcinoma. *Cancer Prev. Res.* **13**, 911–922 (2020).
26. Heinrich, B. et al. Steatohepatitis impairs T cell-directed immunotherapies against liver tumors in mice. *Gastroenterology* **160**, 331–345.e6 (2021).
27. Dudek, M. et al. Auto-aggressive $CXCR6^+$ CD8 T cells cause liver immune pathology in NASH. *Nature* https://doi.org/10.1038/s41586-021-03233-8 (2021).
28. Moeini, A. et al. An immune gene expression signature associated with development of human hepatocellular carcinoma identifies mice that respond to chemopreventive agents. *Gastroenterology* **157**, 1383–1397.e11 (2019).
29. Moscat, J., Karin, M. & Diaz-Meco, M. T. p62 in cancer: signaling adaptor beyond autophagy. *Cell* **167**, 606–609 (2016).
30. Kerdiles, Y. M. et al. Foxo1 links homing and survival of naive T cells by regulating L-selectin, CCR7 and interleukin 7 receptor. *Nat. Immunol.* **10**, 176–184 (2009).
31. Taylor, R. S. et al. Association between fibrosis stage and outcomes of patients with nonalcoholic fatty liver disease: a systematic review and meta-analysis. *Gastroenterology* **158**, 1611–1625.e12 (2020).
32. van der Poorten, D. et al. Hepatic fat loss in advanced nonalcoholic steatohepatitis: are alterations in serum adiponectin the cause? *Hepatology* **57**, 2180–2188 (2013).

Dominik Pfister[1,82], Nicolás Gonzalo Núñez[2], Roser Pinyol[3], Olivier Govaere[4], Matthias Pinter[5,6], Marta Szydlowska[1], Revant Gupta[7,8], Mengjie Qiu[9], Aleksandra Deczkowska[10], Assaf Weiner[10], Florian Müller[1], Ankit Sinha[11,12], Ekaterina Friebel[2], Thomas Engleitner[13,14,15], Daniela Lenggenhager[16], Anja Moncsek[17], Danijela Heide[1], Kristin Stirm[1], Jan Kosla[1], Eleni Kotsiliti[1], Valentina Leone[1,18], Michael Dudek[19], Suhail Yousuf[9], Donato Inverso[20,21], Indrabahadur Singh[1,22], Ana Teijeiro[23], Florian Castet[3], Carla Montironi[3], Philipp K. Haber[24], Dina Tiniakos[4,25], Pierre Bedossa[4], Simon Cockell[26], Ramy Younes[4,27], Michele Vacca[28], Fabio Marra[29], Jörn M. Schattenberg[30], Michael Allison[31], Elisabetta Bugianesi[27], Vlad Ratziu[32], Tiziana Pressiani[33], Antonio D'Alessio[33], Nicola Personeni[33,34], Lorenza Rimassa[33,34], Ann K. Daly[4], Bernhard Scheiner[5,6], Katharina Pomej[5,6], Martha M. Kirstein[35,36], Arndt Vogel[35], Markus Peck-Radosavljevic[37], Florian Hucke[37], Fabian Finkelmeier[38], Oliver Waidmann[38], Jörg Trojan[38], Kornelius Schulze[39], Henning Wege[39], Sandra Koch[40], Arndt Weinmann[40], Marco Bueter[41], Fabian Rössler[41], Alexander Siebenhüner[42], Sara De Dosso[43], Jan-Philipp Mallm[44], Viktor Umansky[45,46], Manfred Jugold[47], Tom Luedde[48], Andrea Schietinger[49,50], Peter Schirmacher[51], Brinda Emu[1], Hellmut G. Augustin[20,21], Adrian Billeter[52], Beat Müller-Stich[52], Hiroto Kikuchi[53], Dan G. Duda[53], Fabian Kütting[54], Dirk-Thomas Waldschmidt[54], Matthias Philip Ebert[55], Nuh Rahbari[56], Henrik E. Mei[57], Axel Ronald Schulz[57], Marc Ringelhan[58,59,60], Nisar Malek[61], Stephan Spahn[61], Michael Bitzer[61], Marina Ruiz de Galarreta[24,62], Amaia Lujambio[24,62,63], Jean-Francois Dufour[64,65], Thomas U. Marron[24,66], Ahmed Kaseb[67], Masatoshi Kudo[68], Yi-Hsiang Huang[69,70], Nabil Djouder[23], Katharina Wolter[71,72], Lars Zender[71,72,73], Parice N. Marche[74,75], Thomas Decaens[74,75,76], David J. Pinato[77,78], Roland Rad[13,14,15], Joachim C. Mertens[17], Achim Weber[16,79], Kristian Unger[18], Felix Meissner[11], Susanne Roth[9], Zuzana Macek Jilkova[74,75,77], Manfred Claassen[7,8], Quentin M. Anstee[4,80], Ido Amit[10], Percy Knolle[19], Burkhard Becher[2], Josep M. Llovet[3,24,81] ✉ & Mathias Heikenwalder[1] ✉

[1]Division of Chronic Inflammation and Cancer, German Cancer Research Center (DKFZ), Heidelberg, Germany. [2]Institute of Experimental Immunology, University of Zurich, Zurich, Switzerland. [3]Liver Cancer Translational Research Laboratory, Institut d'Investigacions Biomèdiques August Pi i Sunyer (IDIBAPS)-Hospital Clínic, Liver Unit, Universitat de Barcelona, Barcelona, Spain. [4]Translational and Clinical Research Institute, Faculty of Medical Sciences, Newcastle University, Newcastle, UK. [5]Division of Gastroenterology and Hepatology, Department of Internal Medicine III, Medical University of Vienna, Vienna, Austria. [6]Liver Cancer (HCC) Study Group Vienna, Medical University of Vienna, Vienna, Austria. [7]Internal Medicine I, University Hospital Tübingen, Faculty of Medicine, University of Tübingen, Tübingen, Germany. [8]Department of Computer Science, University of Tübingen, Tübingen, Germany. [9]Department of General, Visceral and Transplantation Surgery, Universitätsklinikum Heidelberg, Heidelberg, Germany. [10]Department of Immunology, Weizmann Institute of Science, Rehovot, Israel. [11]Experimental Systems Immunology Laboratory, Max-Planck Institute of Biochemistry, Munich, Germany. [12]Institute of Translational Cancer Research and Experimental Cancer Therapy, Klinikum rechts der Isar, Technical University Munich, Munich, Germany. [13]Center for Translational Cancer Research (TranslaTUM), Technical University Munich, Munich, Germany. [14]Department of Medicine II, Klinikum Rechts der Isar, Technical University Munich, Munich, Germany. [15]German Cancer Consortium (DKTK), German Cancer Research Center (DKFZ), Munich, Germany. [16]Department of Pathology and Molecular Pathology, University and University Hospital Zurich, Zurich, Switzerland. [17]Department of Gastroenterology and Hepatology, University Hospital Zurich, Zurich, Switzerland. [18]Research Unit of Radiation Cytogenetics, Helmholtz Zentrum Munich, Munich, Germany. [19]Institute of Molecular Immunology and Experimental Oncology, Technical University Munich, Munich, Germany. [20]Division of Vascular Oncology and Metastasis, German Cancer Research Center (DKFZ-ZMBH Alliance), Heidelberg, Germany. [21]European Center of Angioscience (ECAS), Medical Faculty Mannheim, Heidelberg University, Heidelberg, Germany. [22]Emmy Noether Research Group Epigenetic Machineries and Cancer, Division of Chronic Inflammation and Cancer, German Cancer Research Center (DKFZ), Heidelberg, Germany. [23]Cancer Cell Biology Programme, Growth Factors, Nutrients and Cancer Group, Spanish National Cancer Research Centre, CNIO, Madrid, Spain. [24]Mount Sinai Liver Cancer Program, Division of Liver Diseases, Icahn School of Medicine at Mount Sinai, New York, NY, USA. [25]Department of Pathology, Aretaeion Hospita, National and Kapodistrian University of Athens, Athens, Greece. [26]Bioinformatics Support Unit, Faculty of Medical Sciences, Newcastle University, Newcastle, UK. [27]Department of Medical Sciences, Division of Gastro-Hepatology, A.O. Città della Salute e della Scienza di Torino, University of Turin, Turn, Italy. [28]University of Cambridge Metabolic Research Laboratories, Wellcome-MRC Institute of Metabolic Science, Addenbrooke's Hospital, Cambridge, UK. [29]Dipartimento di Medicina Sperimentale e Clinica, University of Florence, Florence, Italy. [30]Metabolic Liver Research Program, I. Department of Medicine, University Medical Center Mainz, Mainz, Germany. [31]Liver Unit, Department of Medicine, Cambridge Biomedical Research Centre, Cambridge University NHS Foundation Trust, Cambridge, UK. [32]Assistance Publique-Hôpitaux de Paris, Hôpital Beaujon, University Paris-Diderot, Paris, France. [33]Medical Oncology and Hematology Unit, Humanitas Cancer Center, Humanitas Clinical and Research Center-IRCCS, Milan, Italy. [34]Department of Biomedical Sciences, Humanitas University, Milan, Italy. [35]Department of Gastroenterology, Hepatology and Endocrinology, Hannover Medical School, Hannover, Germany. [36]University Medical Center Schleswig-Holstein, Schleswig-Holstein, Germany. [37]Department of Internal Medicine and Gastroenterology (IMuG), Hepatology, Endocrinology, Rheumatology and Nephrology including Centralized Emergency Department (ZAE), Klinikum Klagenfurt am Wörthersee, Klagenfurt, Austria. [38]Department of Gastroenterology, Hepatology and Endocrinology, University Hospital Frankfurt, Frankfurt, Germany. [39]Department of Internal Medicine, Gastroenterology & Hepatology, University Medical Center Hamburg-Eppendorf, Hamburg, Germany. [40]Department of Internal Medicine, University Medical Center of the Johannes Gutenberg University Mainz, Mainz, Germany. [41]Department of Surgery and Transplantation, University Hospital Zurich, Zurich, Switzerland. [42]Department of Medical Oncology and Hematology, University Hospital Zurich and University of Zurich, Zurich, Switzerland. [43]Oncology Institute of Southern Switzerland, Bellinzona, Switzerland. [44]Division of Chromatin Networks, German Cancer Research Center (DKFZ) and Bioquant, Heidelberg, Germany. [45]Clinical Cooperation Unit Dermato-Oncology, German Cancer Research Center (DKFZ), Heidelberg, Germany. [46]Department of Dermatology, Venereology and Allergology, University Medical Center Mannheim, Ruprecht-Karl University of Heidelberg, Heidelberg, Germany. [47]Core Facility Small Animal Imaging, German Cancer Research Center Heidelberg, Heidelberg, Germany. [48]Department of Gastroenterology, Hepatology and Infectious Diseases, Medical Faculty, Heinrich-Heine-University, Düsseldorf, Germany. [49]Immunology Program, Memorial Sloan Kettering Cancer Center, New York, NY, USA. [50]Immunology and Microbial Pathogenesis Program, Weill Cornell Graduate School of Medical Sciences, New York, NY, USA. [51]Institute of Pathology, University Hospital Heidelberg, Heidelberg, Germany. [52]Department of General, Visceral and Transplantation Surgery, Heidelberg University Hospital, Heidelberg, Germany. [53]Edwin L. Steele Laboratories for Tumor Biology, Department of Radiation Oncology, Massachusetts General Hospital, Boston, MA, USA. [54]Department of Gastroenterology and Hepatology, University of Cologne, Cologne, Germany. [55]Department of Medicine II, Medical Faculty Mannheim, Heidelberg University, Heidelberg, Germany. [56]Department of Surgery at University Hospital Mannheim, Medical Faculty Mannheim, Heidelberg University, Heidelberg, Germany. [57]Mass Cytometry Lab, Deutsches Rheumaforschungszentrum Berlin, a Leibniz Institute, Berlin, Germany. [58]Institute of Virology, Technical University Munich/Helmholtz Zentrum Munich, Munich, Germany. [59]Department of Internal Medicine II, University Hospital rechts der Isar, Technical University Munich, Munich, Germany. [60]German Center for Infection Research (DZIF), partner site Munich, Munich, Germany. [61]Medical University Hospital Department of Internal Medicine I, Tübingen, Germany. [62]Department of Oncological Sciences, Icahn School of Medicine at Mount Sinai, New York, NY, USA. [63]The Precision Immunology Institute, Icahn School of Medicine at Mount Sinai, New York, NY, USA. [64]University Clinic for Visceral Surgery and Medicine, Inselspital, Bern, Switzerland. [65]Hepatology, Department of Biomedical Research, University of Bern, Bern, Switzerland. [66]Department of Medicine, Division of Hematology/Oncology, Tisch Cancer Institute, Mount Sinai Hospital, New York, NY, USA. [67]Department of Gastrointestinal Medical Oncology, The University of Texas MD Anderson Cancer Center, Houston, TX, USA. [68]Department of Gastroenterology and Hepatology, Kindai University Faculty of Medicine, Osaka-, Sayama, Japan. [69]Institute of Clinical Medicine, National Yang-Ming University, Taipei, Taiwan. [70]Division of Gastroenterology and Hepatology, Taipei Veterans General Hospital, Taipei, Taiwan. [71]Department of Medical Oncology and Pneumology (Internal Medicine VIII), University Hospital Tübingen, Tübingen, Germany. [72]Cluster of Excellence 'Image Guided and Functionally Instructed Tumor Therapies' (iFIT), Eberhard-Karls University of Tübingen, Tübingen, Germany. [73]German Consortium for Translational Cancer Research (DKTK), Partner Site Tübingen, German Cancer Research Center (DKFZ), Tübingen, Germany. [74]Université Grenoble Alpes, Grenoble, France. [75]Institute for Advanced Biosciences, Research Center UGA/Inserm U 1209/CNRS 5309, Grenoble, France. [76]Service d'hépato-gastroentérologie, Pôle Digidune, CHU Grenoble Alpes, Grenoble, France. [77]Department of Surgery & Cancer, Imperial College London, Hammersmith Hospital, London, UK. [78]Division of Oncology, Department of Translational Medicine, University of Piemonte Orientale, Novara, Italy. [79]Institute of Molecular Cancer Research (IMCR), University of Zurich, Zurich, Switzerland. [80]Newcastle NIHR Biomedical Research Centre, Newcastle upon Tyne Hospitals NHS Trust, Newcastle, UK. [81]Institució Catalana de Recerca i Estudis Avançats (ICREA), Barcelona, Spain. [82]Present address: Liver Disease Research, Global Drug Discovery, Novo Nordisk A/S, Malov, Denmark. ✉e-mail: jmllovet@clinic.cat; m.heikenwaelder@dkfz-heidelberg.de